Crystal Defect and Dislocation Analysis of SiC Wafers by Transmission Polarization Microscopy

TAKENAKA, Kensuke* TAWARA, Takeshi* KATO, Tomohisa‡

ABSTRACT

4H-SiC single crystal wafers need to be analyzed carefully because they still have a higher crystal defect density than silicon wafers. As a method for non-destructive evaluation of crystal defects, synchrotron radiation x-ray topography is mainly used in a large synchrotron radiation facility, where is, however, not easily used. Therefore, as a non-destructive and convenient method for evaluating crystal defects in SiC wafers, we examined a technique for observing strain inside crystals caused by crystal dislocation using transmission polarization microscopy. This method is expected to be used in the detailed analysis of crystal dislocation that has been difficult by synchrotron radiation x-ray topograph alone, in acceptance inspections of commercially-available SiC epitaxial wafers, and in inspections of SiC device manufacturing processes.

1. Introduction

4H silicon carbide (SiC) single crystal wafers need to be analyzed carefully because they still have a crystal defect density that is higher than the single crystal silicon (Si) wafers used for power devices. Therefore, the evaluation of crystal defects is important in terms of device characteristic degradation and quality control. X-ray topography is mainly used as a non-destructive method for evaluating crystal dislocation*1 in single crystal wafers. However, X-ray topography apparatus that uses normal X-ray sources do not provide enough sensitivity to detect all dislocations due to insufficient X-ray strength and resolution. Therefore, for more detailed analysis, synchrotron radiation X-ray topography using large synchrotron radiation facilities is used so that higher brightness and parallelisms can be obtained. However, large-scale synchrotron radiation facilities require an enormous amount of energy. Therefore, they are limited in terms of usage period and are not easy to use. Therefore, it has been necessary to develop a simpler and more convenient method for evaluating crystal defects.

In this paper, we discuss the results of studied about evaluating crystal defects in a non-destructive and simple single crystal SiC wafer using transmission polarization microscopy as an alternative method to synchrotron radiation X-ray topography.

*1: Crystal dislocation: Atoms are arranged regularly in crystals. Crystal dislocation is a crystal defect in which deviation in the atoms is linear.

* National Institute of Advanced Industrial Science and Technology (AIST) (seconded from Fuji Electric)

‡ National Institute of Advanced Industrial Science and Technology (AIST)

2. Technological Background of Evaluation Method for SiC Crystal Defects by Using Transmission Polarization Microscopy

X-ray topography captures the X-ray diffraction strain caused by the elastic strain created by crystal dislocation as an X-ray topograph. The resolution of synchrotron radiation X-ray topography is around 1 μm due to the limitation of two-dimensional detectors such as nuclear emulsion plates.

On the other hand, birefringence (i.e., double refraction) occurs when stress is applied to a material possessing optical anisotropy or to an optically isotropic material. It is commonly recognized that when birefringence is observed in a single crystal material using a polarizing microscope, the phase differential (which is a function of the thickness) is observed as a strain field. Single crystal gadolinium gallium garnet (GGG: $Gd_3Ga_5O_{12}$), a material used in the field of optics, has a large birefringence due to photoelasticity. As a result, it is recognized that the strain field due to crystal dislocation of GGG is easy to observe using a polarizing microscope. Furthermore, it has been reported that the birefringence pattern obtained by simulating threading screw dislocation (TSD) and threading edge dislocation (TED) coincides with the actual transmission polarization image of GGG[(1)].

However, since single crystal SiC only has a small birefringence due to its hardness, only transmission polarization images of birefringence patterns due to the large defects such as micropipes (MP) had been reported[(2)-(3)]. Subsequently, Ma, et al. reported in 2003 the results of comparing the transmission polarization images of a single crystal 6H-SiC bulk wafer*2 with

*2: Bulk wafer: An SiC single crystal ingot is obtained in the low-temperature region by sublimating raw-material SiC with heat. The wafer is cut out of this ingot.

synchrotron radiation X-ray topographs[4]. However, the method for evaluating SiC crystal dislocation using transmission polarization observations did not spread. Although Blasi, McGuire et al. referred to the research of Ma et al. in their work, they mainly utilized the polarization microscopy for only MP examination methods[5]. This tendency is considered to be due to the fact that the observation conditions under which SiC crystal dislocations are easily observed, or the correlation between the birefringence pattern due to the SiC crystal dislocation and the simulation was not sufficiently discussed.

3. Effect of Diffusion Light from Source in Transmission Polarization Observation

Typical transmission type optical microscopes use an optical system that condenses white light with a condenser lens, and then irradiates the sample with radial diffused light and also receives transmitted light radially on the objective lens side.

However, when optically observing the strain field due to crystal dislocation in material with small birefringence due to the photoelasticity like single crystal SiC, the light source itself becomes a cause of significant reduction of image quality when irradiating radially diffused light. Figure 1(a) shows a transmission simplified polarization image when observing a high quality n-type 4H-SiC bulk wafer with an MP density of $<1/cm^2$ with an optical microscope using a general optical system. Almost no other small strain fields are observed around the MP defect[6].

In contrast, the crystal dislocation detector microscope XS-1 manufactured by Mipox Corporation uses a monochromatic UV-LED light source with a central wavelength of 405 nm. Additionally, XS-1 irradiates the sample with collimated linearly polarized light by passing it through a polarizer via a 405 ±10 nm bandpass filter. As shown in Fig. 1(c), high-sensitivity is achieved by controlling the diffusion light from the source. Figure 1(b) shows the transmission polarization image captured by this apparatus[6]. Many small strain fields are observed around the MP defect. Considering the MP density of SiC wafer, it is considered that these small strain fields originate from crystal dislocations.

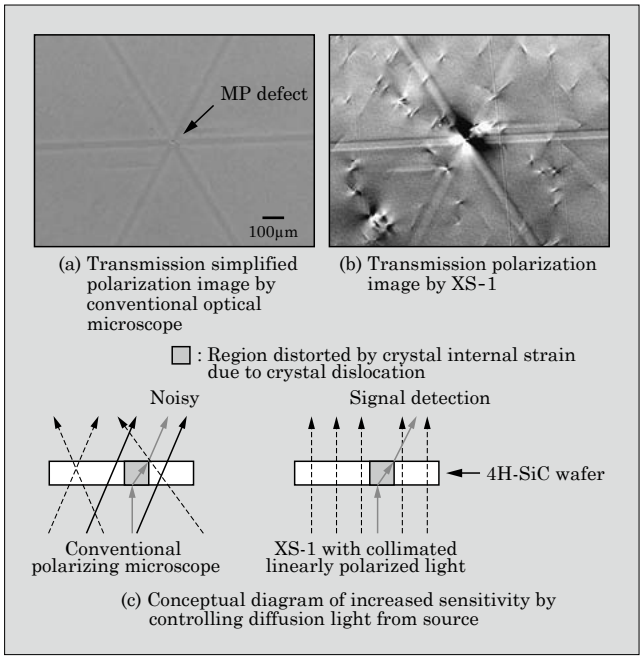

Fig.1 Effect of diffusion light from source in transmission polarization observation

4. Effect of the Roughness of the Polarized Light Incidence Surface and Back Surface in Transmission Polarization Observation

In transmission polarization microscopy, fine irregularities on the front and back surfaces reduce in image quality if the surface state of wafer is roughly finished. Table 1 shows the results of evaluating the effect of the surface roughness of the polarized light incidence surface at approximately the same position on the wafer. An n-type SiC bulk wafer with a chemical mechanical polishing (CMP) finished on the Si-face and a mirror finished on the C-face has a clear transmission polarization image when linear polarization is irradiated from the Si-face side. However, it can be seen that the image quality of transmission polarization image is reduced when incidence occurs from the C-face. On the basis of this result, it can be seen that the effect of the surface roughness on the incidence surface side of linearly polarization light tends to be larger. However, if the C-face has a matte finished surface, it becomes completely noisy and nothing can be observed as

Table 1 Effect of the roughness of the polarized light incidence surface and back surface in transmission polarization observation

Surface finish	Incidence surface of polarization Si-face	Incidence surface of polarization C-face
Si-face CMP C-face mirror	(a) 	(b) 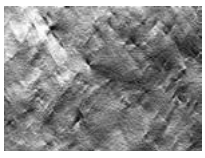
Si-face CMP C-face matte	(c) 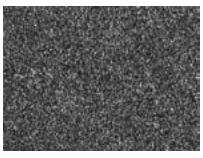	(d) 
Double-sided CMP	(e) 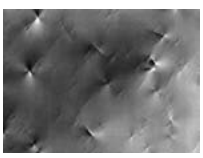	(f) 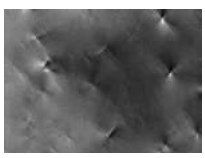

shown in Table 1(c).

Furthermore, the degree of haze [= scattered light/total optical transmitted light × 100 (%)] was examined for another n-type SiC bulk wafer with an Si-face CMP finished and C-face mirror finished by using JASCO Corporation's V-770 UV-visible-near infrared spectrophotometer with ISN-923 integrating sphere unit. The degree of haze at Si-face incidence and C-face incidence were measured to be about 0.04% at wavelengths of 200 to 850 nm. On the basis of this result, we found that there was not enough difference in diffusion transmission to detect the CMP finished surface and mirror finished surface and that just a very little amount of light scattering reduce the quality of transmission polarization image.

5. Comparison of Synchrotron Radiation X-ray Topograph and Transmission Polarization Image About SiC Bulk Wafer

Figure 2(a) shows the C-face side synchrotron radiation X-ray topograph of a high quality n-type SiC bulk wafer with a thickness of 350 μm and MP density of $<1/cm^2$, double-sided CMP finished. Nuclear emulsion plate was used for the two-dimensional detector. X-ray wavelength was 0.15 nm and diffraction condition of $g = 11\bar{2}8$. Figure 2(b) shows the transmission polarization image by the XS-1 at approximately the same position. The strain by the six TSDs X-ray diffraction observed in the upper right corner of the synchrotron radiation X-ray topograph was generally consistent with the position of the strain field in the transmission polarization image. It is assumed that the TSD periphery becomes optically strained due to the crystal internal strain caused by the stress of TSD. Therefore, by controlling the diffusion light from the source, we found that the transmission polarization microscope can observe with a sensitivity comparable to synchrotron radiation X-ray topography. Synchrotron radiation X-ray topography observes the crystal internal strain as an X-ray topograph only based on the diffracted beam satisfying the X-ray diffraction conditions in the region of synchrotron radiation incidence. In contrast, transmission polarization images are seemed to provide a greater amount of information since all crystal internal strain in the depth direction of the wafer is observed. If the information in the depth direction of transmission polarization images becomes able to analyze, it must be helpful to improving failure analysis technology of SiC devices.

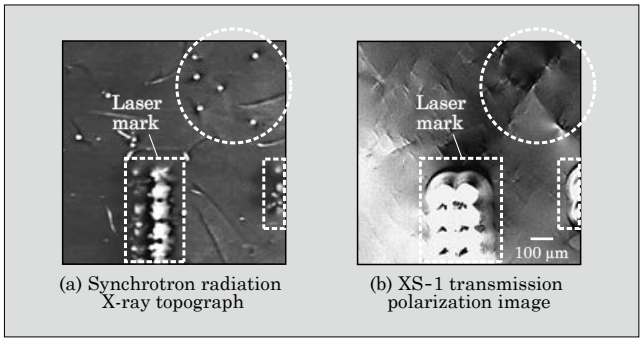

Fig.2 Example of comparative evaluation n-type SiC bulk wafer

6. Identification of Crystal Dislocation by Using SiC Self-Standing Epitaxial Wafers*3,*4

6.1 Experimental production of SiC self-standing epitaxial wafer

We tried to identify crystal dislocation types more closely by comparing synchrotron radiation X-ray topograph and XS-1 transmission polarization images. When doing so, we considered that an n-type SiC bulk wafer would not necessarily be suitable for detailed comparison since it is susceptible to complicated crystal internal strain in the depth direction due to high-speed crystal growth. Furthermore, we considered that light absorption loss originating from highly doped nitrogen will be unfavorable because it interferes with transmission polarization observations.

In consideration of the issues of n-type SiC bulk wafers into account, we investigated the identification method of crystal dislocation types by using a higher quality, low carrier concentration SiC self-standing epitaxial wafer. At first, we grew n+ buffer layer and n- thick layer with target carrier concentration of $4 \times 10^{14}/cm^3$ and target thickness 275 μm in continuity on the Si-face of a commercially available 4°-off 350 μm thick n-type SiC bulk wafer. Next, all n-type SiC bulk wafer and n+ buffer layer were removed by grinding and polishing, as shown in Fig. 3(a), we experimentally produced a double sided CMP finished SiC self-standing epitaxial wafer with a residual thickness of about 240 μm. Figure 3(b) shows the photograph of 15 mm square SiC self-standing epitaxial wafer. Due to the low carrier concentration, it was almost colorless and translucent.

6.2 Comparison of the synchrotron radiation X-ray topograph and transmission polarization image

Figure 3(c) shows the synchrotron radiation X-ray topograph of the SiC self-standing epitaxial wafer, and Fig. 3(d) shows the transmission polarization image at almost the same position. About TSD and TED, the positions of dislocation contrasts of synchrotron radiation X-ray topograph are almost identical with

*3: Epitaxial wafer: This is a wafer in which a thin film is formed (epitaxial growth) on a bulk wafer, etc. in alignment with the crystal surface of the wafer.

*4: Self-standing epitaxial wafer: This is a wafer consisting entirely of epitaxial film obtained by forming an epitaxial film of sufficient thickness in the epitaxial wafer and then removing the bulk wafer component through grinding and polishing.

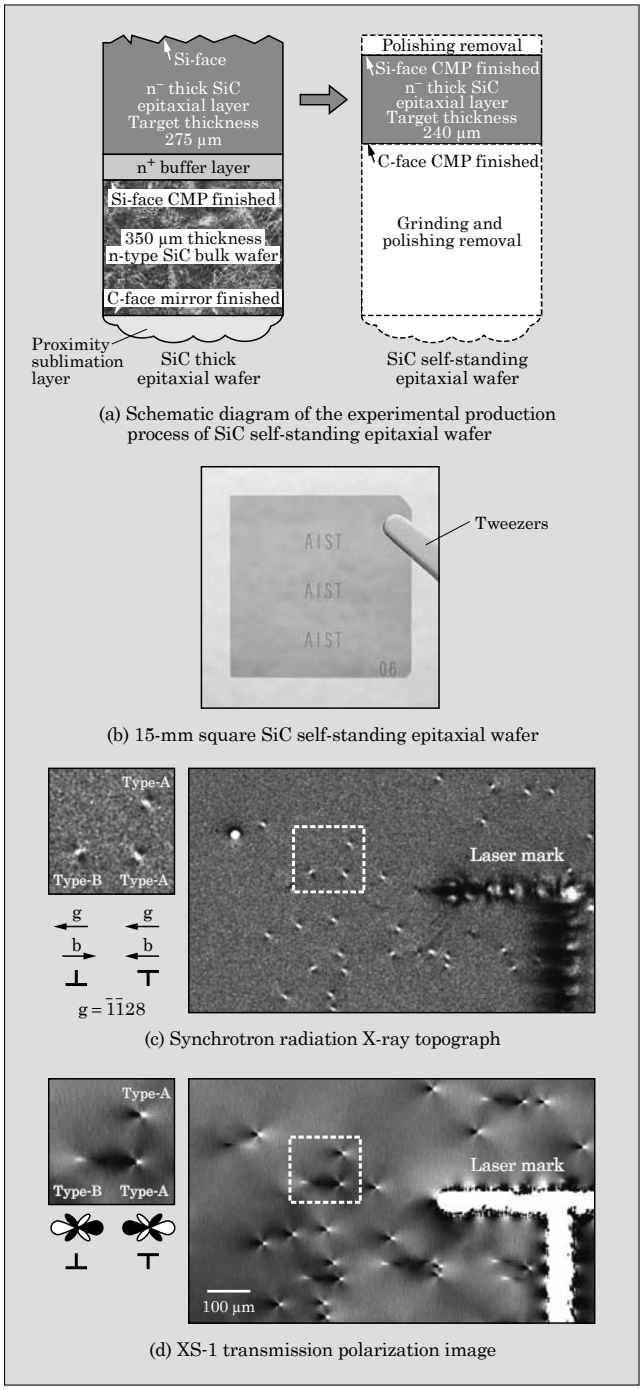

Fig.3 Evaluation of dislocations by using SiC self-standing epitaxial wafer

the positions of birefringence pattern of transmission polarization image. In the SiC self-standing epitaxial wafer, threading dislocations can be observed in a more well-ordered state. Furthermore, the TED birefringence pattern of the transmission polarization images was roughly classified into Type-A or Type-B. The TED dislocation contrast in SiC epitaxial film has been reported to be classified into six categories based on the orientation of the Burgers vector b[7]. Therefore, we considered that the difference between Type-A and Type-B is based on the orientation of the TED Burgers vector b. In particular, Type-A had the similar shape as the TED birefringence pattern shown in the simulation of single crystal GGG. Note that the XS-1 performs phase differential signal processing with black and white inversion of the birefringence pattern. Therefore, the fast and slow birefringence vibration directions are displayed inversely against commonly used transmission polarization microscopy images. As result, the direction of dislocation lines become the direction shown in the schematic diagram of the birefringence pattern of Fig. 3(d).

In addition, the birefringence pattern of Type-B TED is seemingly different from the TED birefringence pattern shown in single crystal GGG simulation. But when observing the SiC self-standing epitaxial wafer tilted in a direction that eliminates the off-angle, we have confirmed a phenomenon in which the Type-B birefringence pattern approaches the Type-A birefringence pattern shape with appearances. From this result, we considered that the birefringence pattern of Type-B TED differing due to the influence of the off-angle.

On the other hand, various birefringence patterns were observed for TSD as shown in Table 2. Type-C had the same shape as the TSD birefringence pattern shown in the simulation of single crystal GGG. But Type-D was inverted 180° relative to Type-C.

In addition, we also confirmed that there are dislocations containing TED components in the bi-

Table 2 Comparison of SiC dislocation contrast and birefringence pattern about SiC self-standing epitaxial wafer

Synchrotron radiation X-ray topograph Dislocation contrast	XS-1 transmission polarization image Birefringence pattern	Remarks
Large	Type-C	This type is similar to the TSD shown in the single crystal GGG computer simulation.
	Type-D	This type is similar to the TSD shown in the single crystal GGG simulation, but it inverts the Type-C 180°.
	Type-E	This is a TSD type that also has a edge dislocation component. It has the possibility of demonstrating threading mixed dislocation (TMD).
	Type-F	These are examples of TSD. It is difficult to evaluate. It shows various birefringence patterns.
Medium	Type-G	This type has clearly smaller dislocation contrast than TSD, but shows a different birefringence pattern than TED.

refringence pattern of the transmission polarization image, although it is clearly observed as TSD in the synchrotron radiation X-ray topograph. We consider that these dislocations are threading mixed dislocation (TMD) that have both characteristic of TSD and TED[6]. It is difficult to identify TMD with synchrotron radiation X-ray topograph alone, but by using the transmission polarization observation method together, it may be probably possible to analyze the detailed of the TSD dislocation contrast of the synchrotron radiation X-ray topograph.

On the other hand, the TSD shown in Type-F showed a variety of birefringence patterns. It is considered that it is necessary to further increase the number of evaluations and introduce simulation analysis. Furthermore, medium-sized dislocations clearly smaller than the TSD shown in Type-G did not correspond with the birefringence pattern of TED and were difficult to identify by using synchrotron radiation X-ray topograph alone. From this result, it would be necessary to consider the introduction of another evaluation method for identifying Type-G.

7. Evaluation of Basal Plane Dislocation by Transmission Polarization Observation

7.1 Evaluation of basal plane dislocation using by single crystal sapphire wafer

As can be seen from Fig. 2, because the dislocation line extends in the horizontal direction of the wafer and the phase difference is small, the basal plane dislocation (BPD) has a problem that the detection sensitivity by transmission polarization observation is low. The 15-mm square SiC self-standing epitaxial wafer that we experimentally produced was characterized by low light absorption loss and was suitable for BPD observation. However, BPD was not observed in the synchrotron radiation X-ray topograph. We estimated that all BPDs were converted to TED by the epitaxial growth of the n^+ buffer layer.

Therefore, we performed a comparison with transmission polarization images (see Fig. 4 for an example) for a single crystal sapphire wafer [Surface orientation: c-face (0001); thickness 350 µm; double-side CMP finished] that is considered suitable for BPD observation due to the higher transmittance in the ultraviolet band than single crystal SiC wafers. We used Rigaku Corporation's XRT-300 X-ray topography system (Mo kα ray, diffraction condition of $g = 11\bar{2}0$) for imaging the transmission X-ray topograph of sapphire wafer. The curved pattern observed in the transmission polarization image in Fig. 4(b) corresponded with the curved strain due to BPD observed in the transmission X-ray topograph in Fig. 4(a). However, BPD from left to right was not observed for the observation surface in Fig. 4(b), although it was observable when the wafer was rotated by 45° counterclockwise with respect to the observation surface in Fig. 4(b). This tendency is considered to be due to the effect of the extinction level at 45° angle against the analyzer in the transmission polarization images.

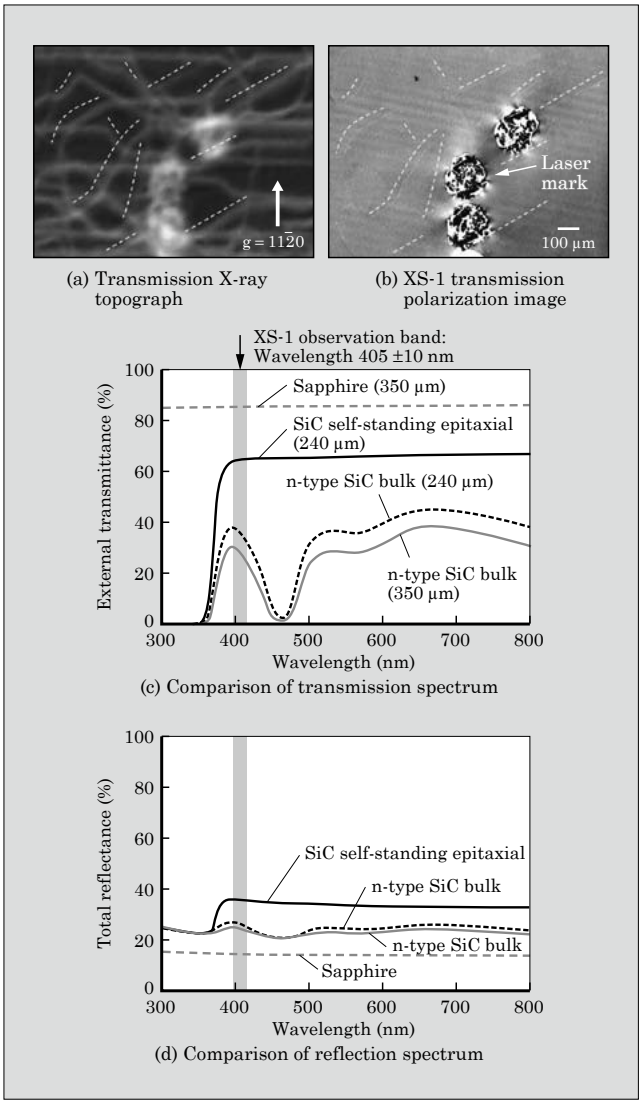

Fig.4 Evaluation of basal plane dislocation(BPD) by using sapphire wafer

7.2 Comparison of single crystal SiC and sapphire about optical properties

Figures 4(c) and 4(d) show the transmission spectrum and reflection spectrum measured with the V-770 UV-visible-near infrared spectrophotometer with ARMN-920 absolute reflectance measurement unit. Note that the external transmittance (%) is the relative transmittance when the air transmittance is 100%. Furthermore, total reflectance (%) is measured as relative reflectance when the reflectance of an aluminum mirror is 100%. In addition, the value of total reflectance is obtained by correcting the measured value of reflection spectrum by the theoretical reflectivity of aluminum.

The external transmittance at a center wavelength

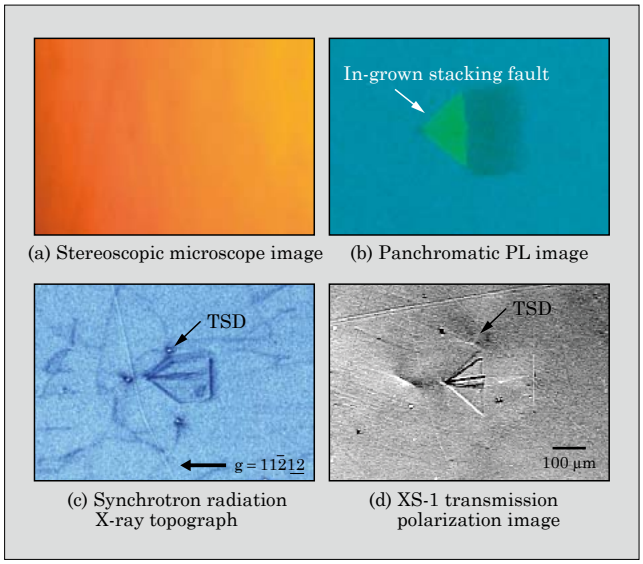

Fig.5 Evaluation example of stacking faults in SiC epitaxial film by transmission polarization image

of 405 nm in the observation band of XS-1 was highest for the sapphire at about 85%, followed by the SiC self-standing epitaxial wafer at about 64% and 350 μm thick n-type SiC bulk wafer at about 28%.

On the other hand, the total reflectance (specular reflectance + diffuse reflectance) at a wavelength of 405 nm was about 15% for sapphire and about 36% for the SiC self-standing epitaxial wafer, whereas the internal transmittance [= External transmittance/(100 – total reflectance) × 100 (%)] of the material itself excluding reflection loss was nearly 100% for both. On the other hand, the total reflectance of the n-type SiC bulk wafer was about 25% and the internal transmittance about 38%. More than half of the incident light was lost as absorption loss in the bulk wafer, possibly causing low sensitivity to BPD. Improvement of the UV-LED light source power and introduction of the more lower loss optical system are considered to be important remaining issues.

8. Evaluation Example of Stacking Faults in SiC Epitaxial Film by Transmission Polarization Image

The XS-1 can also observe the transmission polarization image of an SiC epitaxial wafer if the back side has a mirror finished surface (see Fig. 5). In-grown stacking faults in the epitaxial film of commercially available SiC epitaxial wafers are not visible in the stereoscopic microscope image. However, in the XS-1 transmission polarization image, stacking faults and peripheral threading screw dislocations can both be observed. Furthermore, it was also possible to observe the crystal internal strain due to threading dislocations after performing $3 \times 10^{20}/cm^3$ aluminum ion implantation on the surface of the SiC epitaxial film and activation annealing.

Therefore, transmission polarization observation may be useful as an acceptance inspection method for SiC epitaxial wafers and as an inspection method during SiC device manufacturing processes.

9. Postscript

In this paper, we described crystal defect and dislocation analysis for SiC single crystal wafers using transmission polarization microscopy. In particular, we evaluated crystal dislocation in single crystal SiC wafers that affect the reliability of SiC devices by using commercially available n-type SiC bulk wafers, SiC self-standing epitaxial wafers and commercially available SiC epitaxial wafers. As a result, we proposed a nondestructive and simple crystal defect evaluation method using transmission polarization microscopy. If a wafer inspection system is developed that is equipped with a polarization optics system supporting this evaluation method, it may be possible to perform crystal defect inspection with ease at manufacturing facilities and laboratories having the same accuracy as large synchrotron radiation facilities.

The SiC-wafer crystal defect evaluation method by using transmission polarization microscopy and synchrotron radiation X-ray topographs described in this paper were obtained through the cooperation of Dr. Yoshiyuki Yonezawa, Dr. Hirotaka Yamaguchi and Dr. Hajime Okumura in National Institute of Advanced Industrial Science and Technology (AIST). In addition, the XS-1 SiC crystal dislocation detector microscope used in this paper was developed for this research by Mr. Seiji Mizutani in Vision Psytec with the cooperation of Mr. Kenji Nakagawa in Mipox Corporation. Part of this research was supported by Council for Science, Technology and Innovation(CSTI), Cross-ministerial Strategic Innovation Promotion Program (SIP), "Next-generation power electronics/Consistent R&D of next-generation SiC power electronics" (funding agency: NEDO)

References

(1) Ming, Nai-ben: Ge, Chuan-zhen. Direct observation of defects in transparent crystals by optical microscopy. Journal of Crystal Growth 1990, vol.99, p.1309-1314.
(2) Takahashi, J. et al. Institute of Physics conferenceseries. No. 137, Silicon Carbide and Related Materials (1994) p.13.
(3) Kato, T. et al. Materials Science and Engineering: B. The photoelastic constant and internal stress around micropipe defects of 6H-SiC single crystal. 1999, vol.57, p.147-149.
(4) Ma, X. et al. Extended SiC Defects: Polarized Light Microscopy Delineation and Synchrotron White-Beam X-Ray Topography Ratification. Japanese Journal of Applied Physics. 2003, vol.42, L1077-L1079.
(5) Blasi, R. et al. International Conference on Silicon-

Carbide and Related Materials 2017 (ICSCRM2017), WE.CP.7.
(6) Kato, T. et al. International Conference on Silicon-Carbide and Related Materials 2017 (ICSCRM2017), WE.BP.6.
(7) Kamata, I. et al. Materials Science Forum. Vols. 645-648 (2010), p.303-306.

Fuji Electric

Innovating Energy Technology